

Non-thermal X-ray Emission from Merging Massive Black Hole Binaries

Luke Major Krauth¹* and Jordy Davelaar^{2,3}

¹*Gravitation Astroparticle Physics Amsterdam (GRAPPA), University of Amsterdam, Science Park 904, 1098 XH Amsterdam, The Netherlands*

²*Department of Astrophysical Sciences, Peyton Hall, Princeton University, Princeton, NJ 08544, USA*

³*NASA Hubble Fellowship Program, Einstein Fellow*

Accepted XXX. Received YYY; in original form ZZZ

ABSTRACT

Recent hydrodynamical simulations have identified a disappearing thermal X-ray signature in massive black hole binaries (MBHBs) embedded in circumbinary disks, arising from the tidal truncation and depletion of minidisks shortly before merger. This feature has been proposed as a promising electromagnetic counterpart to MBHB mergers detectable by LISA. In this work, we examine whether non-thermal X-ray emission powered by magnetic reconnection could obscure or modify this thermal X-ray drop. We construct semi-analytic models for both the thermal X-ray emission from minidisks and the non-thermal synchrotron emission produced by reconnection in magnetically dominated black hole magnetospheres. Evaluating these models across the MBHB mass range relevant for LISA, we find that for physically motivated magnetic field strengths and accretion rates, the non-thermal X-ray luminosity remains several orders of magnitude below the thermal component throughout the inspiral. Even under optimistic assumptions that enhance the non-thermal emission, it remains significantly subdominant. We further incorporate the magnetospheric balding framework to model the decay of non-thermal emission near merger, finding that reconnection-powered X-ray emission fades on short, mass-scaled timescales once the external magnetic flux supply is disrupted. Taken together, our results indicate that non-thermal emission is unlikely to mask the disappearing thermal X-ray signature, reinforcing its robustness as an electromagnetic counterpart to MBHB mergers and its potential utility for multi-messenger studies with LISA.

Key words: accretion, accretion discs – black hole physics – hydrodynamics – magnetic reconnection

1 INTRODUCTION

The cores of most galaxies are thought to host a massive black hole (MBH) (Lynden-Bell 1969). When galaxies merge, it is expected that the MBHs in each will slowly sink towards each other, eventually becoming gravitationally bound, forming a massive black hole binary (MBHB) (Begelman et al. 1980).

The gas around this MBHB is expected to turn into a thin disk supported by angular momentum (Prendergast & Burbridge 1968; Pringle & Rees 1972; Shakura & Sunyaev 1973). Numerical simulations over the last decades have commonly found similar aspects of these MBHB+ CBD systems. As the binary orbits, a low density, elongated central cavity is carved into the CBD (Artymowicz & Lubow 1996; MacFadyen & Milosavljevic 2008; Shi et al. 2012; Ragusa et al. 2016). Additionally, material is tidally stripped from the closest edge of the cavity wall, and forms into streams that feed the BHs. Smaller discs, commonly called “minidisks” can form around each BH from some of this infalling gas. Meanwhile, other portions of the stream are flung out towards the far end of the cavity and can build into a non-axisymmetric density commonly called the “lump.” Once every several binary orbits this lump itself leads to flow patterns around the cavity wall

which ultimately modulate the accretion onto the binary (Shi et al. 2012; D’Orazio et al. 2013; Noble et al. 2021; Krauth et al. 2023, 2025). Any of these regions, streams, CBD, lump, minidisks, as well as their interplay, can lead to observable signatures (Westernacher-Schneider et al. 2022).

Amongst this chaos, Krauth et al. (2023) recently found a promising EM signature—a disappearing thermal X-ray luminosity that presents in many MBHB systems just before merger. Using 2D hydrodynamical simulations at high resolution, Krauth et al. (2023) observed that within these MBHB+CBD systems, the minidisks surrounding each BH are responsible for the most energetic photon emission, which falls primarily in the X-ray band. In the late, GW-dominated inspiral, the minidisks become tidally truncated, leading to reduced surface area and a corresponding reduction in both their accretion rates and luminosity. As the system approaches merger, in the last hours/days, this loss is so great that there is a several-order of magnitude drop in the thermal X-ray luminosity.

The accretion rate drop responsible for the X-rays’ disappearance was also found in isothermal gas models (Dittmann et al. 2023). Additionally, the X-ray drop was confirmed for 3D hyper-Lagrangian resolution simulations with up to 2.5th-order Post-Newtonian (PN) corrections (Franchini et al. 2024), intermediate mass ratio inspirals (IMRIs) (Clyburn

* E-mail: L.M.KRAUTH@uva.nl

& Zrake 2024), for certain models which depended on binary torque (Zrake et al. 2025), and unequal-mass binaries with $0.1 \leq q = M_2/M_1 \leq 0.5$ (Krauth et al. 2025).

Not only could this distinct signature lead to sky localization of host galaxies of MBHB mergers in the LISA error volume, but it could also open new avenues for scientific results. From gravitational waves of these systems, observations can provide detailed information about the component masses, orbital parameters, spin characteristics, and luminosity distance of the MBHB (Bogdanovic et al. 2022). The EM counterparts to the systems can provide us information on the spectral energy distribution (SED), periodic variability, jet orientation, and also orbital parameters (Baker et al. 2019; Bogdanovic et al. 2022). When combining this information, one can constrain the speed of gravitational waves (Haiman et al. 2009), test General Relativity against alternative theories (de Rham et al. 2018; Hassan & Rosen 2012), provide a relation between merging MBHs and their host galaxies as a function of redshift, luminosity and other properties, allowing us to better understand the co-evolution of MBHs with their host galaxies (Kormendy & Ho 2013), as well as gain insight into the primary mechanisms driving the mass growth of MBHs over cosmic epochs (see, e.g., Baker et al. 2019; Bogdanovic et al. 2022 for reviews and references). As such, understanding the potential EM signatures originating from the CBD gas is paramount for these scientific goals.

While many studies have now confirmed this X-ray drop, these works have focused on examining the *thermal* X-ray emission. X-ray emission can however also originate from non-thermal sources. One source potentially relevant to the X-ray drop is that which originates from magnetic reconnection.

When the magnetic pressure near the horizon of a black hole becomes comparable to the ram pressure of the inflowing gas, the accretion flow is expected to enter a magnetically arrested disk (MAD) state (Narayan et al. 2003; Tchekhovskoy et al. 2011). In this regime, strong magnetic flux accumulates near the horizon, inhibiting further inflow and promoting magnetic reconnection in the inner magnetosphere.

During the very late inspiral and early post-merger of a MBHB+CBD system, the progressive depletion of the minidisks and accompanying decline in accretion rate may naturally drive the system toward such a magnetically dominated state (Most & Wang 2024). Global GRMHD simulations of MADs show that strongly magnetized flows generically develop thin current sheets near the black holes, where magnetic reconnection can efficiently convert magnetic energy into non-thermal particle acceleration and high-energy radiation (Ripperda et al. 2020; Chashkina et al. 2021; Ripperda et al. 2022). This process is capable of producing luminous synchrotron emission extending into the X-ray and soft- γ -ray bands.

As the system evolves through merger and the inflow of magnetic flux diminishes, reconnection can rapidly dissipate the large-scale magnetic fields threading the black holes, leading to a “balding” of their magnetospheres (Bransgrove et al. 2021). The associated high-energy emission would then decay on short timescales, potentially producing a brief non-thermal flare followed by rapid fading.

These considerations suggest that a merging MBHB+CBD system may exhibit a short-lived burst of non-thermal X-ray or soft- γ emission coincident with the disappearance of the thermal X-ray signal from the minidisks. Whether such a non-

thermal flare can temporarily obscure or modify the thermal X-ray drop identified by Krauth et al. (2023) remains an open question. Addressing this possibility is the primary goal of this work.

Our main result suggests that, across all realistically feasible regions of parameter space, the non-thermal X-ray component from synchrotron radiation should be several orders of magnitude lower than the emission from the thermal X-ray signature; hence, the disappearing thermal X-ray signature should still survive as a viable means for identifying host galaxies of MBHB mergers.

The remainder of this paper is organized as follows. In § 2, we outline our semi-analytic models for thermal and non-thermal X-ray emission, including the treatment of magnetospheric balding. In § 3, we compare the resulting luminosity scalings and decay timescales across the LISA mass range. In § 4, we summarize our conclusions and discuss observational implications.

2 THERMAL, NON-THERMAL, AND BALDING MODELLING

2.1 Thermal X-ray Emission from Minidisks

We compute the total thermal X-ray luminosity by constructing a smooth, semi-analytic model spectrum whose shape and normalization are informed by the hydrodynamical simulations of Krauth et al. (2023). The simulated spectra motivate both the characteristic thermal peak and the overall spectral shape of the emission originating from the minidisks. We then scale this spectrum with the total binary mass, allowing the peak energy and amplitude to shift according to physically motivated mass dependences consistent with thin-disk emission, while optionally permitting spin-dependent corrections to the radiative efficiency (though spin is not included in our fiducial results).

For each mass, the resulting spectral energy distribution νL_ν is converted to L_ν and integrated over the X-ray band to obtain the total thermal X-ray luminosity,

$$L_X = \int_{E_{\min}}^{E_{\max}} L_E dE, \quad (1)$$

where we adopt an X-ray energy range of $E_{\text{X-ray}} = 0.124\text{--}124.0\text{ keV}$. This procedure preserves the spectral trends seen in the simulations while enabling a controlled extrapolation across the LISA MBHB mass range, providing the thermal X-ray baseline against which we compare non-thermal emission.

2.2 Non-thermal synchrotron model from magnetic reconnection

To model the non-thermal X-ray emission powered by magnetic reconnection, we adopt a semi-analytic synchrotron framework calibrated to reproduce the reconnecting-current-sheet spectra shown in Fig. 2 of Hakobyan et al. (2023). In this picture, relativistic electrons and positrons accelerated during reconnection are described by a power-law distribution with an exponential cutoff,

$$N(\gamma) \propto \gamma^{-p} \exp(-\gamma/\gamma_c), \quad (2)$$

where the spectral index p and cutoff Lorentz factor γ_c are chosen to match the kinetic simulation results in the radiative

reconnection regime. The synchrotron emissivity is computed using the standard angle-averaged synchrotron kernel, integrating over particle energy and pitch angle to obtain the spectral energy distribution νL_ν .

Radiative losses are incorporated following the reconnection-powered synchrotron model of [Hakobyan et al. \(2023\)](#), in which synchrotron cooling limits the characteristic emission frequency through the synchrotron burnoff condition. In practice, this is implemented by allowing the cooling constraint to enter only through the effective critical synchrotron frequency $\nu_c(\gamma, B)$, while leaving the overall emissivity amplitude undamped. This treatment captures the key result from first-principles kinetic simulations that particle acceleration at reconnection X-points remains efficient even in the strong-cooling regime, while the emitted spectrum develops a high-energy cutoff that is largely insensitive to the magnetic field strength.

For a given magnetic field B , the resulting synchrotron spectrum is normalized such that the total radiated power equals a fixed fraction of the available jet power. We parameterize this normalization by assuming that a fraction

$$L_{\text{rec}} = f_{\text{rec}} L_{\text{BZ}} \quad (3)$$

of the Blandford–Znajek jet power L_{BZ} is dissipated through magnetic reconnection and radiated, with f_{rec} taken to be an order-unity efficiency consistent with kinetic reconnection studies and the finding that radiative reconnection converts an $\mathcal{O}(10\%)$ fraction of the Poynting flux into radiation ([Sironi & Spitkovsky 2014](#); [Hakobyan et al. 2023](#)). The corresponding non-thermal X-ray luminosity is obtained by integrating the spectrum over the same $E_{\text{X-ray}} = 0.124\text{--}124.0$ keV band. We evaluate the reconnection-powered spectrum across the MBHB mass range by computing $B(M, \dot{M})$ and the corresponding L_{BZ} at each point in a (M, \dot{M}) grid.

We do not assume a fixed reconnecting volume (e.g. R_{ISCO}^3); instead, we normalize the non-thermal component by an energetic budget $L_{\text{rec}} = f_{\text{rec}} L_{\text{BZ}}$, where the relevant near-horizon scale is already implicit in the Blandford–Znajek power. At larger jet scales, the declining magnetic field strength with radius reduces the available magnetic energy density, shifting dissipation to spatially extended regions and favouring broadband, lower-energy emission. We therefore do not explicitly model non-thermal emission from jet–jet interactions during merger, which are expected to contribute as a slowly varying background rather than to the compact X-ray luminosity relevant for assessing the robustness of the thermal X-ray drop ([Gutiérrez et al. 2024](#)).

In magnetically arrested accretion flows, the near-horizon magnetic field strength B can be related to the dimensionless horizon magnetic flux ϕ_B ; however, we retain B as an explicit parameter here to remain consistent with the calibrated reconnection–synchrotron framework adopted from kinetic simulations. Magnetic field strengths and accretion rates are drawn from physically motivated ranges expected for MAD-like accretion flows, and variations around a fiducial model are used to bracket plausible extremes. The explicit equations and fiducial parameter choices entering this procedure are summarized in Appendix § A.

2.3 Magnetospheric balding and decay of non-thermal emission

To model the decay of the non-thermal X-ray emission once the external magnetic flux supply diminishes, we adopt the magnetospheric “balding” framework developed by [Bransgrove et al. \(2021\)](#). In this picture, magnetic flux threading the black hole event horizon is removed through plasmoid-mediated magnetic reconnection once the external supply of flux diminishes. General-relativistic kinetic and resistive MHD simulations show that the horizon-threading magnetic flux decays quasi-exponentially in time, with a characteristic e-folding timescale set by the reconnection rate in the equatorial current sheet ([Bransgrove et al. 2021](#); [Ripperda et al. 2020, 2022](#)).

In kinetic (collisionless) plasma simulations, appropriate for highly magnetized black hole magnetospheres, the decay timescale is found to be $\tau \sim 100 r_g/c$, while resistive MHD simulations yield somewhat longer timescales, $\tau \sim 300\text{--}500 r_g/c$ (see Fig. 3 of [Bransgrove et al. 2021](#)). Importantly, these decay timescales are largely independent of the absolute magnetic field strength, provided the plasma remains in the highly magnetized regime, and instead scale linearly with the gravitational radius of the black hole.

We therefore model the fading of the reconnection-powered synchrotron emission as an exponential decay,

$$L_X^{\text{nth}}(t) \propto \exp(-t/\tau), \quad (4)$$

with τ parametrized as a multiple of r_g/c . Applying this prescription across the MBHB mass range yields a mass-dependent decay time for the non-thermal X-ray signal, allowing us to determine how rapidly the reconnection-powered emission fades relative to the thermal X-ray drop from the minidisks. This provides a physically motivated estimate of whether non-thermal emission can temporally overlap with, or briefly obscure, the disappearing thermal X-ray signature identified by [Krauth et al. \(2023\)](#).

3 RESULTS

Figure 1 compares the mass scaling of the thermal X-ray luminosity from minidisks to the expected non-thermal synchrotron contribution powered by magnetic reconnection. For fiducial, physically motivated choices of the magnetic field strength and accretion rate, the non-thermal synchrotron component lies several orders of magnitude below the thermal X-ray emission across the full MBHB mass range relevant for LISA. Even when the magnetic field strength and accretion rate are increased by an order of magnitude relative to the fiducial model—values that likely represent optimistic, if not extreme, conditions for magnetospheric reconnection—the resulting synchrotron luminosity remains suppressed by $\gtrsim 2$ orders of magnitude compared to the thermal component. Such a separation suggests that the disappearance of the thermal X-ray signal should remain observable and not be obscured by non-thermal emission, although a residual synchrotron contribution at these enhanced levels could in principle be detectable with sensitive X-ray monitoring.

We note that our fiducial thermal model neglects black hole spin, while the non-thermal synchrotron emission is expected to be most efficient for rapidly spinning black holes that can sustain strong magnetospheres. Including spin-dependent

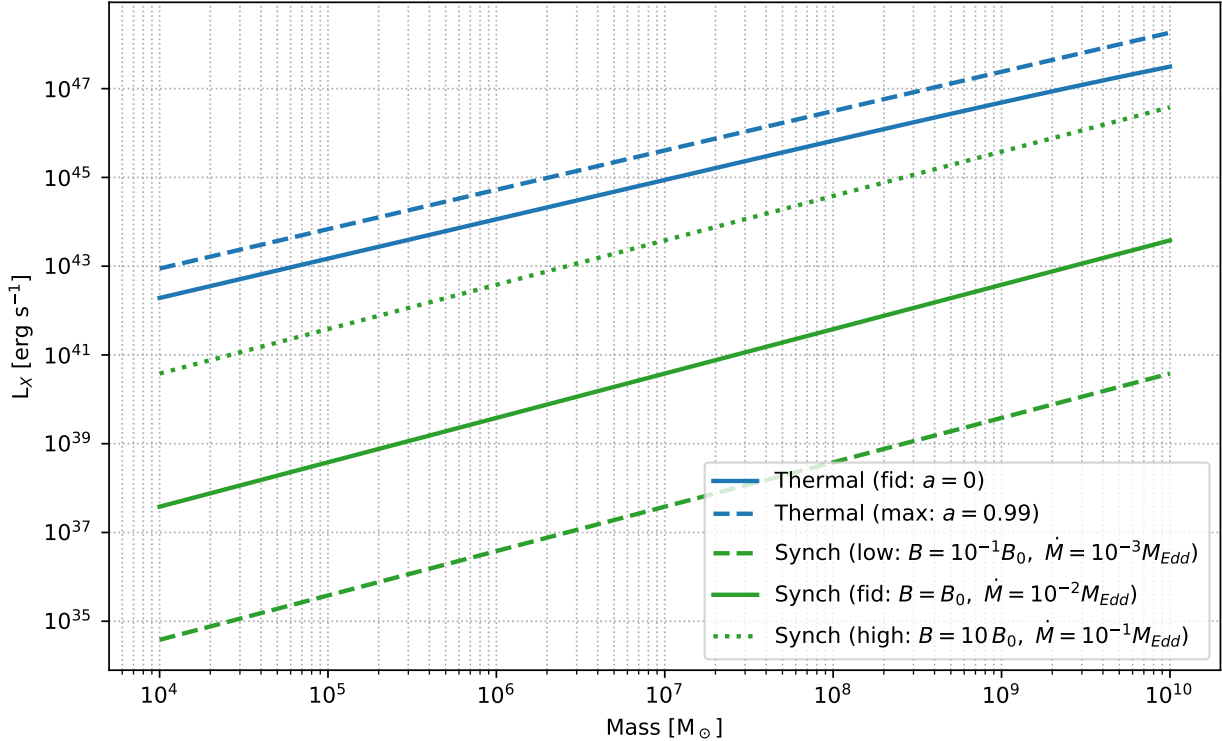


Figure 1. X-ray luminosity L_X as a function of black hole mass for thermal (blue) and synchrotron (green) emission models. Solid and dashed blue curves show the thermal scaling for non-spinning ($a = 0$) and rapidly spinning ($a = 0.99$) black holes, respectively. The green solid curve denotes the fiducial synchrotron model, while dotted and dashed curves illustrate variations with magnetic field strength and accretion rate scaled by factors of 10 and 10^{-1} relative to the fiducial values.

corrections to the thermal radiative efficiency, as illustrated by the $a = 0.99$ thermal model in Fig. 1, further increases the thermal X-ray luminosity and thus accentuates the contrast between the thermal and non-thermal components. This strengthens the conclusion that, even in systems hosting rapidly spinning black holes, the reconnection-powered synchrotron emission is unlikely to mask the pronounced thermal X-ray drop predicted to occur in the final stages of MBHB inspiral.

Figure 2 shows the characteristic timescale on which non-thermal X-ray emission powered by magnetic reconnection is expected to decay once the supply of magnetic flux to the black hole magnetosphere is disrupted. Following the magnetosospheric balding framework of Bransgrove et al. (2021), the luminosity fades quasi-exponentially with an e-folding time $\tau \sim 100\text{--}500 r_g/c$. Because the gravitational timescale scales linearly with black hole mass, the corresponding decay time increases proportionally across the MBHB mass range, from minutes for $M \sim 10^{4\text{--}5} M_\odot$ to days or longer for the most massive systems considered here ($M \sim 10^{9\text{--}10} M_\odot$). Also shown in Fig. 2 is an illustrative timescale for the recovery of thermal X-ray emission following merger. While the precise moment at which the thermal component can be considered ‘‘recovered’’ is not uniquely defined, this curve indicates the time required for the thermal X-ray luminosity to rebound to within approximately two orders of magnitude of its pre-merger level, comparable to even the most optimistic non-thermal contribution considered here. This recovery time remains significantly longer than the reconnection-driven decay time across the full black hole mass range.

As shown in Fig. 1, even pushing the upper bound of what is physically reasonable, the reconnection-powered synchrotron luminosity remains well below the thermal X-ray emission from the minidisks. It can however still be instructive to ask how extreme the physical conditions must be for the reconnection-powered synchrotron emission to approach or exceed the thermal X-ray luminosity from the minidisks. In our framework, this would require both magnetospheric field strengths to be tens of times what is expected for magnetically arrested accretion flows and accretion rates a few to ten times the Eddington limit. Such conditions correspond to an optimistic and likely short-lived corner of parameter space, particularly for MBHBs in the late inspiral phase where the minidisks are simultaneously being depleted. Even under these assumptions, as Fig. 2 indicates, the non-thermal emission would decay rapidly once the external magnetic flux supply diminishes. Consequently, any reconnection-powered non-thermal emission that might transiently compete with the thermal signal before merger is likewise expected to fade, and on a comparatively short timescale, leaving the system X-ray faint in both channels until accretion and magnetic flux are re-established.

4 CONCLUSIONS AND DISCUSSION

In this work, we have investigated whether non-thermal X-ray emission powered by magnetic reconnection could obscure or modify the recently identified disappearing thermal X-ray signature associated with merging massive black hole binaries embedded in circumbinary disks. Motivated by hydro-

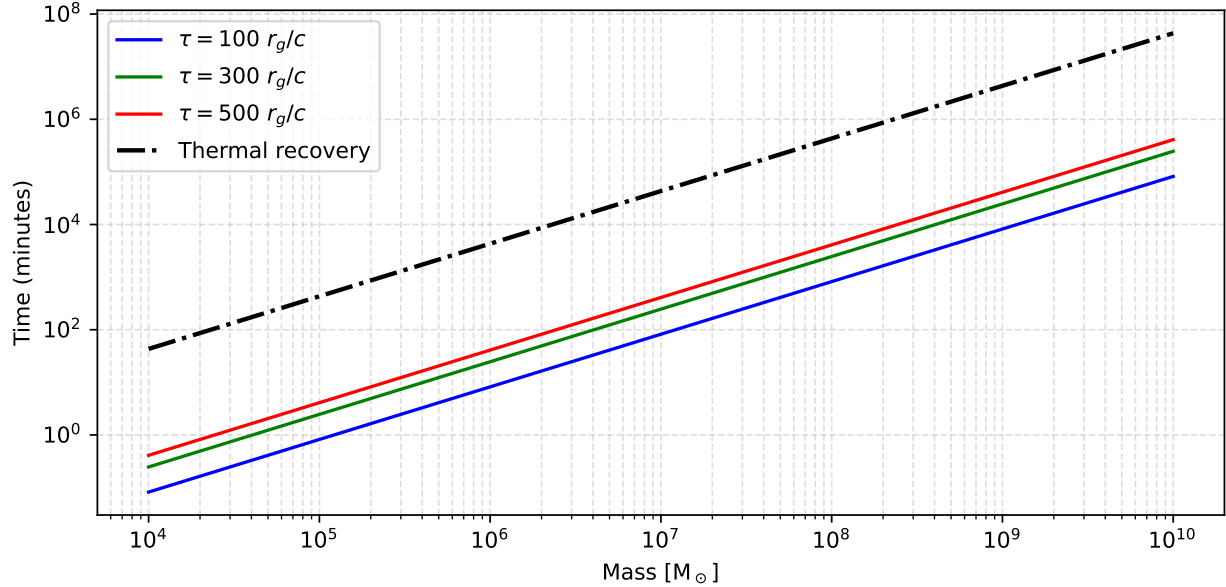


Figure 2. Time required for the non-thermal X-ray luminosity to decay by one e-fold due to magnetospheric balding, shown as a function of black hole mass. Coloured curves correspond to decay timescales $\tau = 100 r_g/c$, $300 r_g/c$, and $500 r_g/c$. The black dash-dotted curve indicates the time required for the thermal X-ray luminosity to recover to within two orders of magnitude of its pre-merger level.

dynamical simulations showing a sharp decline in thermal X-ray emission from tidally truncated minidisks near merger (Krauth et al. 2023), we constructed semi-analytic models for both the thermal and non-thermal components and compared their behaviour across the MBHB mass range relevant for LISA sources.

Our primary result is that, for physically motivated values of the magnetic field strength and accretion rate, the non-thermal synchrotron X-ray luminosity remains several orders of magnitude below the thermal X-ray emission throughout the inspiral. Even when these parameters are pushed to optimistic or extreme values, the non-thermal component remains suppressed by at least ~ 2 orders of magnitude relative to the thermal emission. This indicates that the disappearance of the thermal X-ray signal identified by Krauth et al. (2023) is unlikely to be masked by reconnection-powered synchrotron radiation in realistic astrophysical systems.

Related non-thermal emission channels may also operate in merging MBHB systems, particularly those associated with jet activity on larger spatial scales. For example, models of magnetic reconnection in dual jet-jet interaction regions predict non-thermal radiation originating at distances well beyond the near-horizon magnetosphere (Gutiérrez et al. 2024). In such scenarios, the resulting synchrotron emission is spatially extended, varies slowly, and peaks primarily at infrared to optical/UV energies, with only a modest contribution to the X-ray band even for optimistic acceleration efficiencies. Such emission would therefore act as a quasi-steady luminosity pedestal rather than a rapidly evolving signal tied to the near-merger depletion of the minidisks. As a result, while jet-jet interactions may represent an additional non-thermal channel in MBHB systems, they are unlikely to mask or mimic the compact, merger-associated thermal X-ray drop that is the focus of this work.

While our analysis is designed to capture the order-of-magnitude evolution of the band-integrated thermal X-ray

luminosity, it does not aim to resolve changes to the instantaneous spectral shape during the late inspiral and merger. In particular, magnetic reconnection can accelerate particles into hard power-law distributions, producing non-thermal synchrotron emission that extends into the hard X-ray band, with additional modification at the highest energies possible through Compton upscattering. Because power-law spectra decline more gradually with energy than thermal emission, such non-thermal components could in principle dominate the highest-energy X-ray bands even if they contribute only a small fraction of the total X-ray output. The relative importance of such components depends on the detailed spectral shapes of the thermal and non-thermal emission, and on how they evolve during the final stages of inspiral, which we defer to future work.

We further considered the temporal evolution of the non-thermal emission by incorporating the magnetospheric balding framework of Bransgrove et al. (2021). Once the external supply of magnetic flux diminishes near merger, reconnection rapidly dissipates the horizon-threading magnetic field, causing the non-thermal emission to decay quasi-exponentially on timescales of $\tau \sim 100\text{--}500 r_g/c$. Although this decay time increases linearly with black hole mass, the same mass scaling applies to the duration of the thermal X-ray-dark phase found in hydrodynamical simulations, and to the subsequent recovery of thermal X-ray emission. As a result, even in scenarios where non-thermal emission approaches the thermal level prior to merger, the reconnection-powered component is expected to fade more rapidly than the thermal emission recovers, leaving the system temporarily X-ray dark until accretion and magnetic flux are re-established.

Taken together, these results strengthen the robustness of the disappearing thermal X-ray signature as an electromagnetic counterpart to MBHB mergers. The lack of a long-lived non-thermal contaminant implies that the X-ray-dark phase should provide a clean temporal marker associated

with the final stages of inspiral and merger. Such a signature could play an important role in identifying host galaxies within the LISA localization volume and in coordinating multi-messenger follow-up observations.

Several caveats remain. Our non-thermal model is necessarily idealized and calibrated to kinetic reconnection simulations in simplified geometries, while the true magnetospheric structure of merging MBHBs may be more complex. Magnetic reconnection may also produce inverse-Compton emission, as explored in radiative PIC simulations by [Hakobyan et al. \(2023\)](#). Toward lower black hole masses, the magnetization increases strongly, while the characteristic synchrotron-limited Lorentz factor decreases due to enhanced radiative cooling; at the same time, the characteristic energy of thermal seed photons shifts to higher frequencies for lower-mass systems. The combination of harder seed photons and relativistic pairs therefore places inverse-Compton scattering deep in the Klein–Nishina regime at the low-mass end of our sweep, strongly suppressing IC relative to synchrotron. Efficient IC emission is expected primarily for the highest-mass systems, while radiative PIC simulations further reveal an intermediate spectral excess associated with intermittent plasmoid dynamics. Quantifying the importance of this feature across merger requires fully self-consistent simulations, and we therefore treat any inverse-Compton contribution as a secondary, model-dependent effect. In addition, highly asymmetric systems, extreme spin configurations, or transient episodes of enhanced magnetic flux accumulation could in principle modify the relative balance between thermal and non-thermal emission. We also note that recent 3D GRMHD simulations have shown that, in certain regions of parameter space, accretion onto the binary may persist through merger ([Ennoggi et al. 2025](#)), potentially weakening or delaying the thermal X-ray drop. Future global GRMHD simulations that self-consistently capture both minidisc disruption and magnetospheric reconnection across merger will be essential for fully quantifying these effects.

Nevertheless, within the range of parameters explored here, our results indicate that magnetic reconnection is unlikely to erase or substantially alter the disappearing thermal X-ray signature. Instead, both thermal and non-thermal emission are expected to fade rapidly around merger, reinforcing the picture of a brief but distinct X-ray-dark phase preceding the post-merger re-establishment of accretion. This behaviour underscores X-ray observations as a powerful complement to gravitational-wave detections in probing the final stages of massive black hole binary evolution.

ACKNOWLEDGEMENTS

We acknowledge support from the NWA Roadmap grant “GW LISA/ET: Shivers from the Deep Universe: a National Infrastructure for Gravitational Wave Research” (LK), JD is supported by NASA through the NASA Hubble Fellowship grant HST-HF2-51552.001A, awarded by the Space Telescope Science Institute, which is operated by the Association of Universities for Research in Astronomy, Incorporated, under NASA contract NAS5-26555. *Software:* `python` ([Oliphant 2007](#); [Millman & Aivazis 2011](#)), `scipy` ([Jones et al. 2001](#)), `numpy` ([van der Walt et al. 2011](#)), and `matplotlib` ([Hunter 2007](#)).

DATA AVAILABILITY

The data underlying this article will be shared on reasonable request to the corresponding author.

REFERENCES

Artymowicz P., Lubow S. H., 1996, *The Astrophysical Journal*, **467**, L77

Baker J., et al., 2019, Multimessenger Science Opportunities with mHz Gravitational Waves ([arXiv:1903.04417](#)), [doi:10.48550/arXiv.1903.04417](#)

Begelman M. C., Blandford R. D., Rees M. J., 1980, *Nature*, **287**, 307

Bogdanovic T., Miller M. C., Blecha L., 2022, *Living Reviews in Relativity*, **25**, 3

Bransgrove A., Ripperda B., Philippov A., 2021, *Phys. Rev. Lett.*, **127**, 055101

Chashkina A., Bromberg O., Levinson A., 2021, *Astrophys. J.*, **910**, 37

Clyburn M., Zrake J., 2024, [arXiv e-prints](#), p. [arXiv:2405.10281](#)

D’Orazio D. J., Haiman Z., MacFadyen A., 2013, *Monthly Notices of the Royal Astronomical Society*, **436**, 2997

Dittmann A. J., Ryan G., Miller M. C., 2023, [arXiv e-prints](#), p. [arXiv:2303.16204](#)

Ennoggi L., et al., 2025, *Phys. Rev. D*, **112**, 063009

Franchini A., Bonetti M., Lupi A., Sesana A., 2024, [arXiv e-prints](#), p. [arXiv:2401.10331](#)

Gutiérrez E. M., Combi L., Romero G. E., Campanelli M., 2024, *MNRAS*, **532**, 506

Haiman Z., Kocsis B., Menou K., Lippai Z., Frei Z., 2009, *Classical and Quantum Gravity*, **26**, 094032

Hakobyan H., Ripperda B., Philippov A. A., 2023, *ApJ*, **943**, L29

Hassan S. F., Rosen R. A., 2012, *Physical Review Letters*, **108**, 041101

Hunter J. D., 2007, *Computing in Science and Engineering*, **9**, 90

Jones E., Oliphant T., Peterson P., et al., 2001, SciPy: Open source scientific tools for Python, <http://www.scipy.org/>

Kormendy J., Ho L. C., 2013, *ARA&A*, **51**, 511

Krauth L. M., Davelaar J., Haiman Z., Westernacher-Schneider J. R., Zrake J., MacFadyen A., 2023, *MNRAS*, **526**, 5441

Krauth L. M., Davelaar J., Haiman Z., Westernacher-Schneider J. R., Zrake J., MacFadyen A., 2025, *MNRAS*, **543**, 2670

Lynden-Bell D., 1969, *Nature*, **223**, 690

MacFadyen A. I., Milosavljevic M., 2008, *The Astrophysical Journal*, **672**, 83

Millman K. J., Aivazis M., 2011, *Computing in Science & Engineering*, **13**, 9

Most E. R., Wang H.-Y., 2024, *ApJ*, **973**, L19

Narayan R., Igumenshchev I. V., Abramowicz M. A., 2003, *Publ. Astron. Soc. Japan*, **55**, L69

Noble S. C., Krolik J. H., Campanelli M., Zlochower Y., Mundim B. C., Nakano H., Zilhão M., 2021, *ApJ*, **922**, 175

Oliphant T. E., 2007, *Computing in Science & Engineering*, **9**, 10

Prendergast K. H., Burbidge G. R., 1968, *ApJ*, **151**, L83

Pringle J. E., Rees M. J., 1972, *A&A*, **21**, 1

Ragusa E., Lodato G., Price D. J., 2016, *Monthly Notices of the Royal Astronomical Society*, **460**, 1243

Ripperda B., Porth O., Sironi L., Keppens R., 2020, *Astrophys. J.*, **900**, 100

Ripperda B., Liska M., Chatterjee K., Philippov A. A., Tchekhovskoy A., Markoff S., et al. 2022, *Astrophys. J. Lett.*, **924**, L32

Shakura N. I., Sunyaev R. A., 1973, *Astronomy and Astrophysics*, **24**, 337

Shi J.-M., Krolik J. H., Lubow S. H., Hawley J. F., 2012, *The Astrophysical Journal*, **749**, 118

Sironi L., Spitkovsky A., 2014, *Astrophys. J. Lett.*, **783**, L21
 Tchekhovskoy A., Narayan R., McKinney J. C., 2011, *Mon. Not. R. Astron. Soc.*, **418**, L79
 Westernacher-Schneider J. R., Zrake J., MacFadyen A., Haiman Z., 2022, *Physical Review D*, **106**, 103010
 Zrake J., Clyburn M., Feyan S., 2025, *MNRAS*, **537**, 3620
 de Rham C., Melville S., Tolley A. J., 2018, *Journal of High Energy Physics*, **2018**, 83
 van der Walt S., Colbert S. C., Varoquaux G., 2011, *Computing in Science and Engineering*, **13**, 22

APPENDIX A: FIDUCIAL NON-THERMAL SYNCHROTRON MODEL

This appendix summarizes the equations and fiducial parameters used to compute the reconnection-powered non-thermal X-ray emission discussed in Section 2.2.

The near-horizon magnetic field strength is parameterized as

$$B(M, \dot{M}) = B_0 \left(\frac{M}{10^6 M_\odot} \right)^{-1/2} \left(\frac{\dot{M}}{0.01 \dot{M}_{\text{Edd}}} \right)^{1/2}, \quad (\text{A1})$$

where B_0 is a normalization constant. We adopt a fiducial value $B_0 = 10^5$ G, corresponding to an upper-end realization of reconnection-based magnetospheric models when scaled to MBHB masses and accretion rates. This choice intentionally maximizes the non-thermal synchrotron component, making it more likely to compete with the thermal X-ray emission.

Given $B(M, \dot{M})$, the jet power is taken to scale as

$$L_{\text{BZ}} \propto B^2 M^2, \quad (\text{A2})$$

with spin-dependent factors absorbed into the overall normalization. A fixed fraction of this Blandford–Znajek jet power is assumed to be dissipated and radiated via magnetic reconnection,

$$L_{\text{rec}} = f_{\text{rec}} L_{\text{BZ}}, \quad (\text{A3})$$

where we adopt $f_{\text{rec}} = 0.1$ as a fiducial reconnection efficiency.

The synchrotron spectrum is computed assuming a non-thermal particle distribution

$$N(\gamma) \propto \gamma^{-p} \exp(-\gamma/\gamma_c), \quad (\text{A4})$$

with $p = 1.25$ and $\gamma_c = 5 \times 10^7$. These values are chosen to match kinetic simulations of radiative relativistic magnetic reconnection, which produce hard particle spectra with $1 \lesssim p \lesssim 1.5$ and cutoff Lorentz factors $\gamma_c \sim 10^7$ – 10^8 set by the synchrotron burnoff limit (Hakobyan et al. 2023).